Kinetics and Particle Nucleation Mechanism of St/BA/QBVPBr Emulsifier-Free Cationic Emulsion Polymerization

Jinzhi Zhang, Shiyuan Cheng, Guohong Lu, Shigan Chai

Faculty of Chemistry and Chemical Engineering, Hubei University, Wuhan 430062, China

Received 3 September 2006; accepted 28 July 2008
DOI 10.1002/app.29276
Published online 10 November 2008 in Wiley InterScience (www.interscience.wiley.com).

ABSTRACT: Stable functional cationic latices were prepared by emulsifier-free emulsion copolymerization of styrene (St) and butyl-acrylate (BA) with 1-butyl-4-vinylpyridinium bromide (qBVPBr) as functional comonomer and azobis(isobutyramidine hydrochloride) (AIBA) as initiator at (70 ± 1)°C. The influences of the reaction temperature, the initiator concentration, and comonomer concentration on the polymerization conversion (x %), polymerization rate (R_p) of poly(St/BA/qBVPBr) emulsions were investigated. The results indicated that x % and R_p increase with increasing qBVPBr or AIBA concentration and temperature, and R_p can be expressed as $R_p = K_p[\text{AIBA}]^{0.73}[\text{qBVPBr}]^{0.08}$ ($r_{\text{AIBA}} = 0.9968$; $r_{\text{qBVPBr}} = 0.9946$, both r_{AIBA} and r_{qBVPBr} are linear correlation coefficient) and the apparent activation energy (E_a) is 47.89 kJ mol^{-1}. In the absence of emulsifier condition, curves of R_p versus reaction time obeyed the typical behavior characterized by Intervals I, II, and III as similar conventional emulsion polymerization. The formation and growth of poly(St/BA/qBVPBr) latex particles has been studied at different reaction times. The results indicate that N_p decrease gradually with time at the early polymerization stages and then reach a constant value after about 20% conversion, but D_p by photon correlation spectroscopy grow continuously as all polymerization proceed. Both the particle size distribution and molecular weight distribution curves are of bimodal size distribution and indicate the participation of at least two mechanisms of particle formation, namely, homogeneous nucleation in the aqueous phase and micellar nucleation. © 2008 Wiley Periodicals, Inc. J Appl Polym Sci 111: 2092–2098, 2009

Key words: emulsifier-free cationic emulsion; polymerization rate; kinetics; particle nucleation mechanism

INTRODUCTION

Emulsifier-free emulsions have attracted widespread attentions because of their potential applications. For example, monodisperse latices were used as model systems for studying colloidal stability and for calibrating instruments such as ultracentrifuges and light-scattering units,[1,2] as diagnostics and solid supports for the immobilization of biologically active macromolecules such as antibodies,[3,4] pharmaceuticals drug delivery, immunoassay techniques, and other areas.[5,6]

In the past decades, the mechanism of emulsifier-free emulsion polymerization was widely investigated for almost all the factors that possibly affected polymerization behavior.[7–9] As have been well known, several models regarding the mechanism of particle formation were postulated, namely, micelles nucleation, homogeneous nucleation, and droplets mechanisms. Oligomeric radicals, which generated by the free radical reaction of a water-soluble ionic initiator such as $^{\bullet}S_2O_8^{=}$ from $K_2S_2O_8$, $(NH_4)_2S_2O_8$, or $^{\bullet}C(CH_3)_2C^{+}(NH_2)_2$ from azobis(isobutyramidine hydrochloride) (AIBA) and monomer dissolved in the aqueous phase, associated to form micelles.[10–13] The second is homogeneous nucleation, where oligomers generated in the aqueous phase reached a critical chain length at which they were no longer soluble in the aqueous phase and precipitated to form primary precursor particles[14–16] or a combination of both for the case.[8,17] The others is droplets nucleation, namely, the droplets absorbed the oligomeric radicals generated in the aqueous phase or the interface to continue the polymerization. The monomers transfer from the bulk monomer phase to the growing particles via the coalescence of monomer droplets with particles. The role of reaction in the aqueous phase was just proposed to provide the surface-active oligomer for the stabilization of particles' as well as to promote the colloidal stability of the droplets. The rapid reaction in the aqueous phase due to the high concentration of hydrophilic monomer produced longer hydrophilic chains and led to the coagulation of particles by the nucleation was performed in the droplets.[18,19]

Correspondence to: J. Zhang (zhangjinzhi2000@yahoo.com.cn).

Contract grant sponsor: Hubeishen Education Hall Science Technology Study; contract grant number: D20081003020-096106.

In this study, we report the synthesis of cationic latices prepared by emulsion polymerization of styrene (St) and butyl-acrylate (BA) in presence of the functional cationic comonomer, qBVPBr, and azobis (isobutyramidine hydrochloride) (AIBA) as initiator. A kinetic study of the poly(St/BA/qBVPBr) emulsifier-free emulsion copolymerization is developed with special attention on the effect of the comonomer concentration, AIBA concentration, and temperature on conversions (x %) and the polymerization rate (R_p). The number of particles (N_p), particle size (D_p), particle size distribution (PSD), and the molecular weight distribution (MWD) changed with conversions; Finally, the particle nucleation mechanism was discussed in the presence of water-soluble comonomers.

EXPERIMENTAL

Materials

Styrene (St), butyl acrylate (BA), and 4-vinylpyridine (Janssen Chimica) were distilled under reduced pressure and stored at a refrigerator before use. Azobis(isobutyramidine hydrochloride) (AIBA) was used directly without further purification. The water was deionized grade in all polymerizations. 1-Butyl-4-vinylpyridinium bromide (qBVPBr) was received as a 10% aqueous solution and stored at about 4°C.

Synthesis of 1-butyl-4-vinylpyridinium bromide

1-Butyl-4-vinylpyridinium bromide (qBvpbr) was synthesized in our laboratory by the method described as follows:

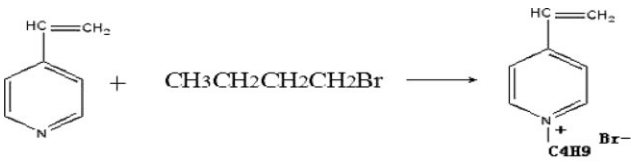

In a 100-mL three-necked, round-bottomed flask with a stirrer, thermometer, and reflux condenser, 6 g 4-vinylpyridine, freshly distilled was mixed with 50 mL acetone, and then 32 g *n*-butyl bromide was added. The reaction was maintained for 12 h at 30°C by stirring during the reaction, and the white precipitated product was obtained from the solution, which was filtered off and washed two to three times with cold acetone. The white crystals were dried under vacuum below 30°C to constant weight and nuclear magnetic resonance (NMR) spectrum was taken to identify the product. Final yield: 46.1%.

The ^{1}H NMR spectra were obtained on a Varian 60 MHz spectrometer. All spectra were determined at ambient probe and on freshly prepared solutions and measured relative to D_2O 4.75, chemical shifts were obtained from SW = 600 Hz and δ as follow:

δ(D_2O): 1.2 (3 H, t, —CH_2—CH_2—CH_2—CH_3^*), 2.4 (4 H, m, —CH_2—CH_2^*—CH_2^*—CH_3), 4.6 (2 H, T, —CH_2^*—CH_2—CH_2—CH_3), 5.8 (2 H, m, —CH=CH_2^*), 6.6 (1 H, m, —CH^*=CH_2), 8.1 (2 *m*-—H, *d*—Ar—H), 9.2 (2 *p*—H, m, Ar—H).

Preparation of poly(St/BA/qBVPBr) soap-free emulsion

Soap-free emulsion polymerizations were conducted using a batch process. All reactants and water, except for the initiator and qBVPBr, were initially charged to a 250-mL four-neck flask equipped with a PTFE-bladed paddle stirrer, a condensation reflux tube, and a centigrade thermometer. St, BA, and deionized water were added to the flask and stirred for about 20 min. The mixture was heated to constant temperature by a thermostat water bath, which was operated at (70 ± 0.1)°C. qBVPBr and AIBA aqueous solution were added to the reactor to start polymerization, simultaneously, starting to count time. The polymerization continued for 6 h at (70 ± 0.1)°C under a nitrogen atmosphere at a stirring rate of 250 rpm. Conversion was measured gravimetrically.

Preparation of polymer sample for the photon correlation spectroscopy

The poly(St/BA/qBVPBr) latex particles were purified by repetitive centrifugation and then redispersed with deionized water to remove water-soluble polymers, free electrolytes, and residual reactants. Then each polymer sample was diluted to about 0.01% solid content Particle hydrodynamic diameters and distribution were measured by photon correlation spectroscopy (PCS) using a Malvern Autosizer Lo-c. The measurements were conducted at room temperature. The number of particles in unit volume of the water (N_p) was calculated by the following equation: $Wx = 1/6\rho\Pi D_p^3 V N_p$, where W is St and BA weight (g), x is St and BA conversion, V is the volume of water (mL), ρ is the polymer density, and D_p is the particle diameter.

The polymerization rates

The R_p (R_p, mol L^{-1} h^{-1}) were deduced from the conversion versus time curves obtained. Then R_p was calculated by equation $R_p = [M] \times dx/dt$, [M] is main monomer (St and BA) total concentration.

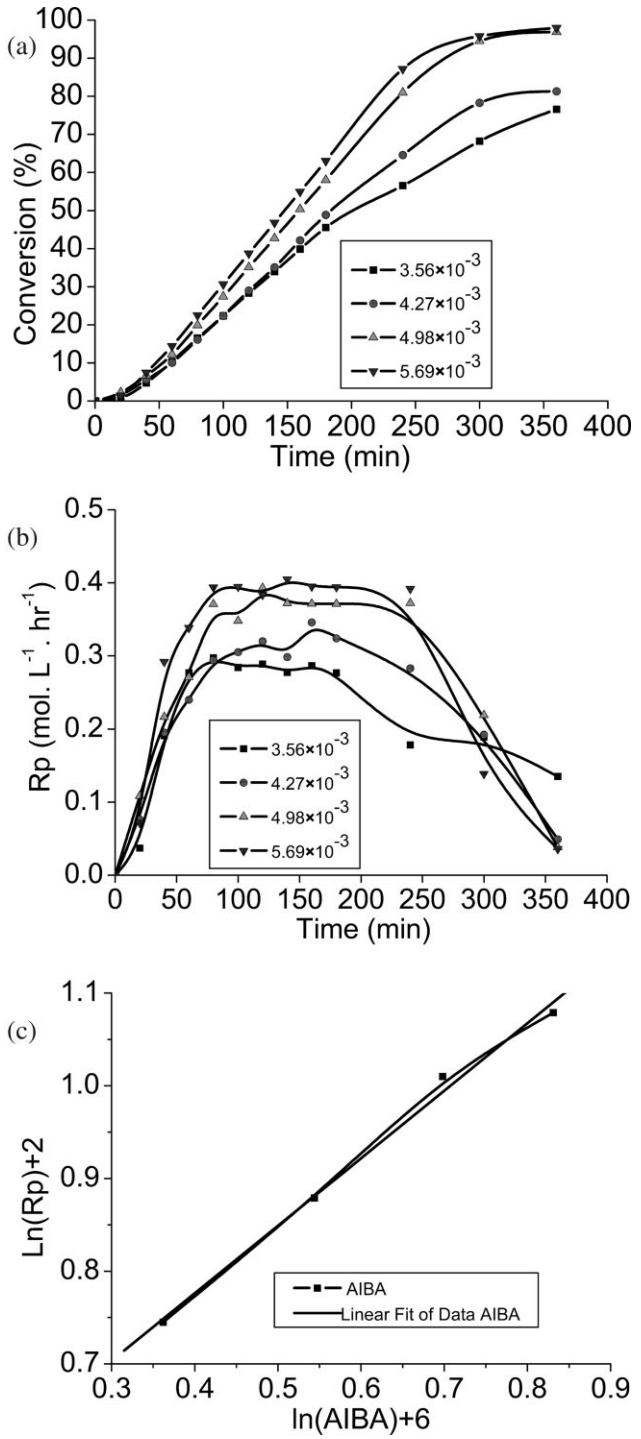

Figure 1 (a) Conversion versus reaction time curves; (b) R_p versus conversion curves; (c) The linear relationship plot between R_p and [AIBA] (rAIBA = 0.9968) at different AIBA concentrations. T=343K Recipe: t/BA/qBVPBr/H_2O=10ml/20ml/1.77×10^{-2}mol.L^{-1}/140mL.

RESULTS AND DISCUSSION

Emulsion polymerization kinetics

To understand how each of the three factors—initiator concentration, comonomer concentration, and temperature—affects the R_p as the other factors remain constant was investigated. Figures 1(a), 2(a), and 3(a) show the effects of the reaction temperature, initiator concentration, and qBVPBr concentration on the conversion during the course of the

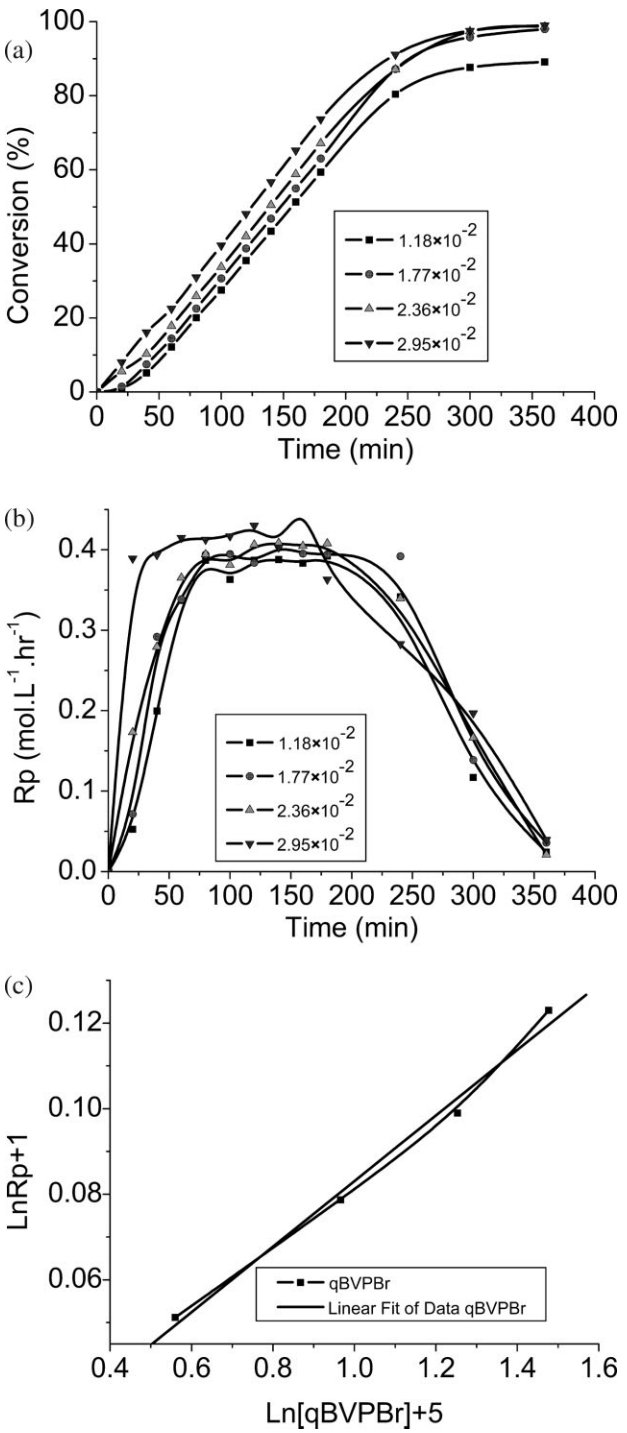

Figure 2 (a) Conversion versus reaction time curves; (b) R_p versus conversion curves; (c) The linear relationship plot between R_p and [qBVPBr] (rqBVPBr=0.9946) at different qBVPBr concentrations. T=343K Recipe: St/BA/AIBA/H_2O=10mL/20mL/5.69×10^{-3}mol.L^{-1}/140mL.

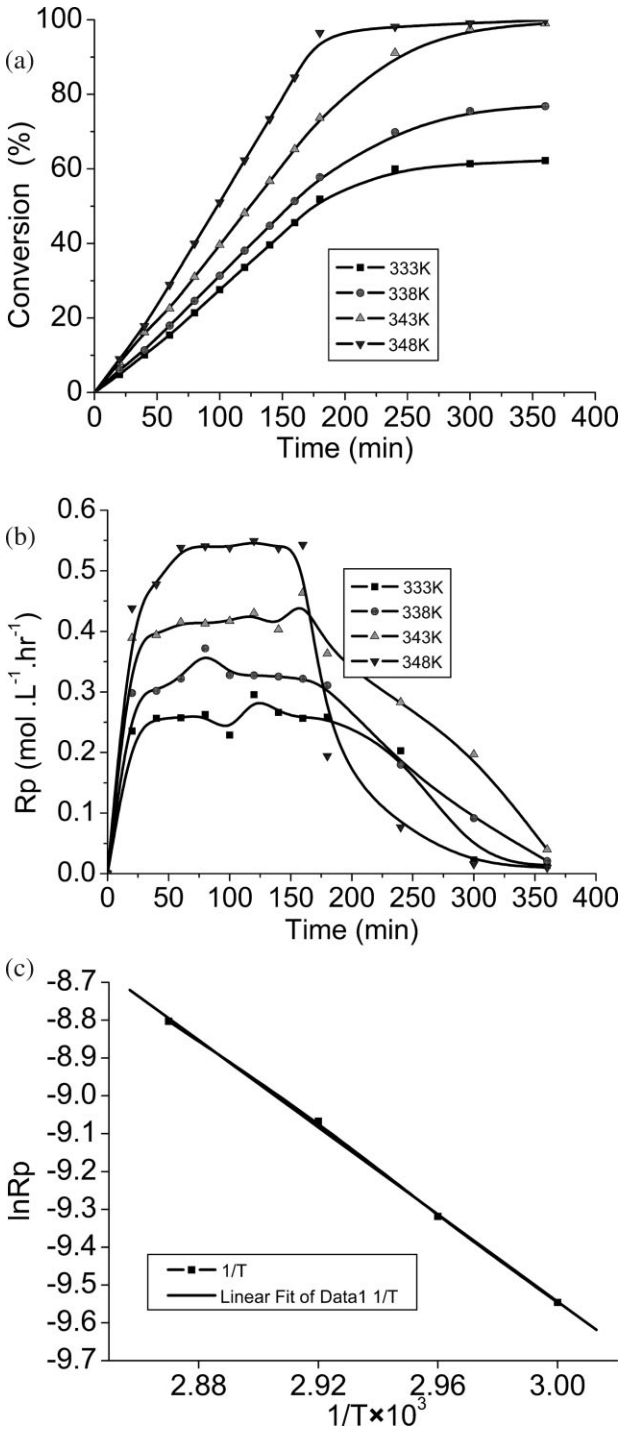

Figure 3 (a) Conversion versus reaction time curves; (b) R_p versus conversion curves; (c) The linear relationship plot between R_p and $1/T$ ($r = -0.9994$) at different temperature. Recipe: St/BA/qBVPBr/AIBA/H_2O=10mL/20mL/2.95×10^{-2}mol.L^{-1}/5.69×10^{-3}mol.L^{-1}/140mL.

reaction. It is observed that the polymerization conversion (x %) increase with temperature, qBVPBr concentration, and AIBA concentration. This is because the higher AIBA concentration and temperature may produce more number of free radicals, and the higher qBVPBr content in the system may produce more oligomer radicals, and more primary particles produced, resulting in enhanced x %.

Another typical representation of the emulsion polymerization kinetics is depicted in Figures 1(b), 2(b), and 3(b), where R_p versus time curves are presented. As shown in Figures 1(b), 2(b), and 3(b), the curves show the Intervals I, II, and III, as expected for this kind of polymerization. The Interval I (R_p, progressively increasing) corresponding to the nucleation period of the particle is observed at conversions lower than about 20%, indicating that the particle nucleation period had ended. Afterward, the Interval II (R_p, constant) associated to an almost constant concentration of monomer inside the growing polymer particles (assuming N_p constant) extends to a conversion near 80%. However, D_p increase with conversion but the monomer droplets decrease. Finally, in the Interval III (R_p, decreasing), the decline of the curve indicate the consumption of the remaining monomer into the growing particles, although the particle number in Interval III remained the same as in Interval II (Fig. 4). The monomer concentration in the particles decrease with conversion and monomer droplets are no longer present; therefore, R_p decrease with the conversion in Interval III.

R_p determined at the Interval II from the curves of Figures 1(b), 2(b), and 3(b) and R_p versus AIBA, qBVPBr concentration, and temperature curves depicted in Figures 1(c), 2(c), and 3(c) were listed in TablesI–III. The results indicate that R_p increase with increasing qBVPBr or AIBA concentration and temperature, and the double logarithmic plot give a regular increasing trend with the order of 0.73 and 0.08 for AIBA and qBVPBr, respectively, and R_p could be expressed as $R_p = K_p[\mathrm{AIBA}]^{0.73}[\mathrm{qBVPBr}]^{0.08}$ ($r_{\mathrm{AIBA}} = 0.9968$; $r_{\mathrm{qBVPBr}} = 0.9946$, both r_{AIBA} and r_{qBVPBr} are linear correlation coefficient). As shown in Figure 3(a–c), temperature has dramatic effect on R_p. An increase in temperature should lead to an

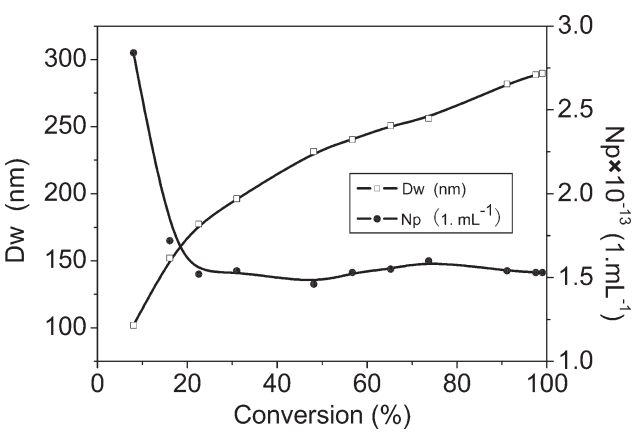

Figure 4 D_p and N_p versus reaction conversion.

TABLE I
Effects of AIBA Concentration on R_p

AIBA $\times 10^3$ (mol/L)	ln[AIBA] + 6	R_p (mol/L h)	ln R_p + 2
3.56	0.362	0.2851	0.745
4.27	0.544	0.3260	0.879
4.98	0.698	0.3716	1.010
5.69	0.831	0.3980	1.079

increase both the decomposition rate of the initiator and the increase of all the rate constants (K_p) and can accelerate the diffusion rate of radicals and monomers. As a result, R_p increase with temperature; with AIBA or qBVPBr concentration increasing, radical concentration increase and lead to R_p increase.

The ln R_p versus $1/T$ curve is shown in Figure 3(c) and is found to be linear with a negative slope ($r = -0.9994$, r is linear correlation coefficient) and the apparent activation energy (E_a) for the conversion was evaluated to be 47.89 kJ mol^{-1} according to the Arrhenius equation.

The growth of latex particles

D_p were measured throughout the course of the polymerization and the variations of N_p with monomer conversion were worked out. The results of particle evolution are showed in Figure 4. Because colloidal stability depends on the particle size and the surface-charge density, colloidal instability will lead to particle coagulation and reduce in the number of particles per unit volume. As can be seen Figure 4, during the early polymerization stage, colloidal instability lead to coagulation, as a result, D_p increase, N_p decrease with time until N_p become constant after about 20% conversion, which indicate that N_p decrease during the nucleation stage and particle nucleation ended before N_p become constant. But D_p grow continuously as all polymerization proceed. After the particle nucleation period, N_p is constant as Figure 4; R_p remain constant until about 80% conversion before the monomer droplets disappear[20] as in Figures 1(b), 2(b), and 3(b).

TABLE II
Effects of qBVPBr Concentration on R_p

qBVPBr $\times 10^2$ (mol/L)	ln[qBVPBr] + 5	R_p (mol/L h)	ln R_p + 1
1.18	0.560	0.3872	0.0512
1.77	0.966	0.3980	0.0787
2.36	1.253	0.4062	0.0990
2.95	1.477	0.4160	0.1230

TABLE III
Effects of Temperature on R_p

T (K)	$1/T \times 10^3$ (1/K)	R_p (mol/L S) $\times 10^5$	ln R_p
333	3.00	7.15	−9.546
338	2.96	8.97	−9.319
343	2.92	11.54	−9.067
348	2.87	15.02	−8.803

Particle size distribution

D_p, N_p versus time plot are shown in Figure 4. As can be seen N_p reaches a constant value after about 20% conversion, D_p grow continuously. It can be noted that the PSD show two well-distinguished fractions of polymer particles only before about 20% conversion corresponding to Interval I in Figure 5, namely, PSD curves are of bimodal size distributions. In addition, PSD peak move toward higher particle diameter domains with increasing conversion, namely, D_p grow continuously during the whole polymerization reaction. PSD curves are of bimodal size distributions; We suggest that the formation of latex particles may occur by two different mechanisms: homogeneous nucleation mechanism and micellar nucleation mechanism similar to that reported in St/BA/DBMEA system.[8] Finally, a monodispense peak is observed; this may be because that the smaller particles had lower surface charge density and were easier to absorb the charged free radicals in the water phase than the larger particles. The smaller particle would grow faster than the larger one. Therefore, the larger and smaller particles compete to grow against each other and finally the particle sizes tend to be uniform, and therefore the degree of monodispersity of the particles increase during growth.

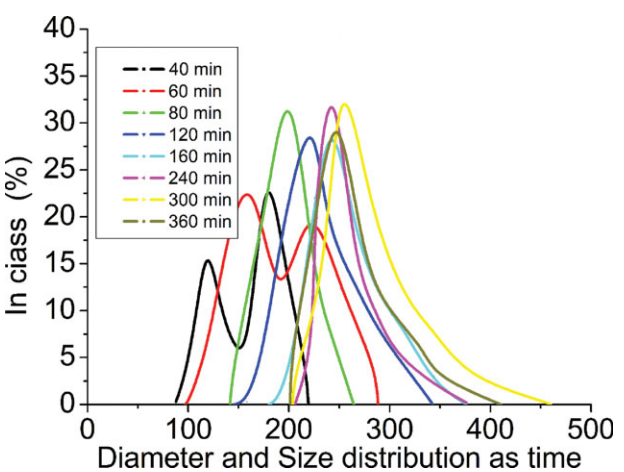

Figure 5 Particle size distributions (PSD) curves versus reaction time. [Color figure can be viewed in the online issue, which is available at www.interscience.wiley.com.]

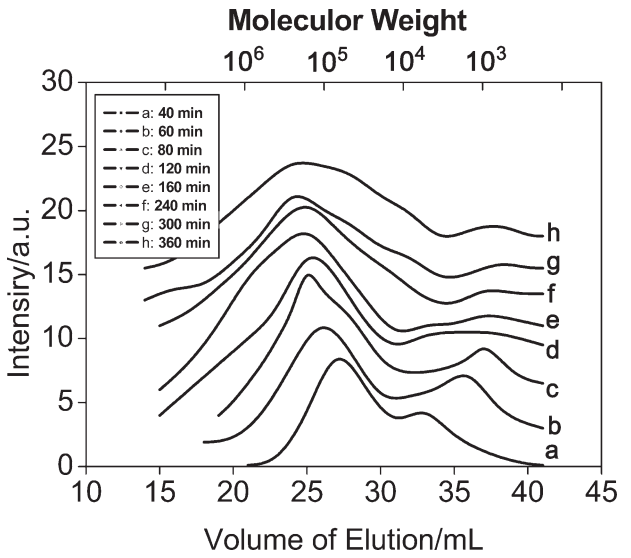

Figure 6 Molecular weight distributions curves (MWD) versus reaction time.

Molecular weight distribution

MWD change as the reaction proceeded in Figure 6. The results show bimodal distribution with the peak of low molecular weight at about 4000 at about 15% conversion in the earlier period.[10,21] As the polymerization proceeds, the amount of low molecular weight polymer decrease in proportion to the total, and the lower MW mode gradually shifts to a higher MW region and grows larger and finally covers the lower MW mode generated in the initial period. As a result, a monodispense distribution is observed as Figure 6. The phenomenon that many molecules of low weight exit in early stage of reaction was also mentioned by Goodpin et al.[11] and Goodall et al.[10] and inspired them to bring forward their micellar type nucleation. In addition, the changing trend of MWD peak is in good agreement with PSD by comparing PSD and MWD experiment results. Therefore, we suggest that there may be micellar nucleation mechanism besides homogeneous nucleation mechanism in the St/BA/qBVPBr polymerization.

Nucleation mechanism

In the case of emulsifier-free emulsion, the presence of the ionic monomer repeat-unit along the copolymer chains could make the mechanism for particle formation more complicated. Several mechanisms have been proposed: micelles nucleation,[10–13] homogeneous nucleation,[8,14] droplets nucleation,[18,22] and so on. It is unlikely that any one of these mechanisms alone would describe particle nucleation for all monomers because the solubility of the monomer and have a large effect on what is, in the initial stages, a process occurring in solution.[23]

For poly(St/BA/qBVPBr) emulsion polymerization without emulsifier, this can be described by the various radical reactions that occur in the aqueous phase at the beginning of the polymerization, which involve radicals originating from initiator decomposition as follows:

$$C^+(NH_2)_2C(CH_3)_2N=N\,C(CH_3)_2C^+(NH)_2 \rightarrow 2^\bullet C(CH_3)_2C^+\,(NH_2)_2(R^\bullet)+N_2$$

$$R^\bullet + M \rightarrow RM^\bullet \quad (M = St, BA, qBVPBr)$$

$$RMMM^{\bullet\bullet\bullet\bullet}M^\bullet + RMMM^{\bullet\bullet\bullet\bullet}M^\bullet \rightarrow RMMM^{\bullet\bullet\bullet\bullet}MM^{\bullet\bullet\bullet}MMMR$$

biomolecular termination

Thermal decomposition of AIBA starts copolymerization of qBVPBr with St and BA in the water phase, copolymerization in the water phase proceeds until the oligomer is captured by already existing particles; the oligomer reaches a critical chain length, after which it will precipitate to form a primary particle, the particles can be generated through homogenous nucleation mechanism; Or at the initial polymer phase, oligomeric radicals reached a critical chain length, at which they became surface active and underwent micellization[10]; The particles can be generated through micelles nucleation mechanism. Therefore, there is a competition between homogenous nucleation and micellar nucleation.

In the St/BA/qBVPBr emulsion polymerization, bimodal distributions of MWD (Fig. 6) and PCS (Fig. 5) are observed in the earlier period and the presence of a peak having about a MW of 4000 indicate that there may be two kinds of nucleation mechanisms, the oligomers of molecular weight of about 4000 behave as emulsifier, simultaneously, water-soluble qBVPBr is able to copolymerize with the main monomers St, BA to form water-soluble oligomeric radicals, which could continuously grow until the oligomer is captured by already existing particles and then coil up and precipitate to form primary particles. Thus, the homogeneous nucleation mechanism is likely to occur.[24,25] After nucleation, the polymerization mainly takes place in the monomer-swollen particles. The radicals in particles are separated, so that the termination of radicals is difficult, and their lifetime is prolonged. Although N_p and R_p remain constant, D_p grows continuous (in Fig. 4).

CONCLUSIONS

Kinetics studies of emulsifier-free emulsion polymerization demonstrate three stages of the polymerization: Interval I at conversion of around 20% and R_p increase; Interval II at conversion of around 80% and R_p keeps constant; and then at the beginning of Interval III R_p decrease rapidly. R_p can be expressed

as $R_p = K_p[\mathrm{AIBA}]^{0.73}[\mathrm{qBVPBr}]^{0.08}$ ($r_{\mathrm{AIBA}} = 0.9968$; $r_{\mathrm{qBVPBr}} = 0.9946$). The PSD and GPC curves show the existence of two fractions of polymer particles. The bimodal PSD and GPC curves suggest the formation of particle by two different mechanisms: one being homogenous nucleation mechanism and the other a micelles nucleation, which occurs mainly in the nucleation interval (Interval I), and the two particle formation mechanisms coexist were in competition in the emulsion polymerization. N_p decrease during the nucleation stage and particle nucleation ended before N_p become constant. But D_p grow continuously as all polymerization proceed.

References

1. Ottewill, R. H.; Haw, J. N. Discuss Faraday Soc 1966, 42, 154.
2. Goodpin, J. W.; Ottwill, R. H.; Pelton, R. Colloid Polym Sci 1979, 257, 61.
3. Delair, T.; Marguet, V.; Pichot, C.; Mandrand, B. Colloid Polym Sci 1994, 272, 962.
4. Fred, T.; Pieter, P.; Anton, L. Eur Polym J 1991, 27, 939.
5. Gonzalez, F. G.; Rodriguez, A. M.; Alvarez, R. H. Colloid Polym Sci 1994, 272, 352.
6. Ruzgas, T. A.; Razumas, V. J.; Kulys; J. J. J Colloid Interface Sci 1992, 151, 136.
7. Lovell, P. A.; El-Aasser, M. S. Emulsion Polymerization and Emulsion Polymers; Wiley: New York, 1997.
8. Zhang, J. Z.; Zou, Q. C.; Li, X. Q.; Cheng, S. Y. J Appl Polym Sci 2003, 89, 2791.
9. Zhang, J. Z.; Cheng, S. Y.; Li, X. Q. Polym Mater Sci Eng 2002, 18, 70.
10. Goodall, A. R.; Wilkinson, M. C.; Hearn, J. J Polym Sci Polym Chem Ed 1977, 15, 2193.
11. Goodpin, J. W.; Hearn, J.; Ho, C. C.; Ottewill, R. H. Br Polym J 1973, 5, 347.
12. Song, Z.; Poehlein, G. W. J Colloid Interface Sci 1989, 128, 486.
13. Song, Z.; Poehlein, G. W. J Colloid Interface Sci 1989, 128, 501.
14. Fitch, R. M. Br Polym J 1973, 5, 467.
15. Feeney, P. J.; Napper, D. H.; Gilbert, R. G. Macromolecules 1984, 17, 2520.
16. Feeney, P. J.; Napper, D. H.; Gilbert, R. G. Macromolecules 1987, 20, 2922.
17. Chen, S. A.; Chang, H. S. J Polym Sci Polym Chem Ed 1985, 23, 2615.
18. Ni, H.; Ma, G.; Nagai, M.; Omi, S. J Appl Polym Sci 2001, 82, 2692.
19. Ni, H.; Ma, G.; Nagai, M.; Omi, S. J Appl Polym Sci 2001, 82, 2679.
20. Gardon, J. L. J Polym Sci Part A-1: Polym Chem 1968, 6, 643.
21. Chang, H. S.; Chen, S. A. J Polym Sci Part A: Polym Chem 1988, 26, 1207.
22. Baxendale, J. H.; Evans, M. G.; Kilham, J. K. Trans Faraday Soc 1946, 42, 668.
23. Fitch, R. M. Polymer Colloids Preprints; NATO Advanced Study Institute: Trondheim, 1975.
24. Liu, I. J.; Krieger, I. M. J Polym Sci Polym Chem Ed 1981, 19, 3013.
25. Van Streun, K. H.; Belt, W. J.; Piet, P.; German, A. L. Eur Polym J 1991, 27, 931.